

Solifluction Processes in an Area of Seasonal Ground Freezing, Dovrefjell, Norway

Charles Harris,^{1*} Martina Kern-Luetsch,¹ Fraser Smith² and Ketil Isaksen³

¹ School of Earth Ocean and Planetary Sciences, Cardiff University, Cardiff, UK

² School of Engineering, University of Dundee, Dundee, UK

³ Norwegian Meteorological Institute, Blindern, Oslo, Norway

ABSTRACT

Continuous monitoring of soil temperatures, frost heave, thaw consolidation, pore water pressures and downslope soil movements are reported from a turf-banked solifluction lobe at Steinhøi, Dovrefjell, Norway from August 2002 to August 2006. Mean annual air temperatures over the monitored period were slightly below 0°C, but mean annual ground surface temperatures were around 2°C warmer, due to the insulating effects of snow cover. Seasonal frost penetration was highly dependent on snow thickness, and at the monitoring location varied from 30–38 cm over the four years. The shallow annual frost penetration suggests that the site may be close to the limit of active solifluction in this area. Surface solifluction rates over the period 2002–06 ranged from 0.5 cm yr⁻¹ at the rear of the lobe tread to 1.6 cm yr⁻¹ just behind the lobe front, with corresponding soil transport rates of 6 cm³ cm⁻¹ yr⁻¹ and 46 cm³ cm⁻¹ yr⁻¹. Pore water pressure measurements indicated seepage of snowmelt beneath seasonally frozen soil in spring with artesian pressures beneath the confining frozen layer. Soil thawing was associated with surface settlement and downslope soil displacements, but following clearance of the frozen ground, later soil surface settlement was accompanied by retrograde movement. Summer rainfall events caused brief increases in pore pressure, but no further soil movement. Surface displacements exceeded maximum potential frost creep values and it is concluded that gelifluction was an important component of slow near-surface mass movements at this site. Temporal and spatial variations in solifluction rates across the area are likely to be considerable and strongly influenced by snow distribution. Copyright © 2008 John Wiley & Sons, Ltd.

KEY WORDS: solifluction; frost heave; thaw settlement; seasonally frozen ground; pore pressures

INTRODUCTION

In this paper we report field measurements of solifluction at Steinhøi, Dovrefjell, Norway (latitude 62° 15' 28" N, longitude 09° 51' 58" E, altitude 1396 m, Figure 1), where seasonal ground freezing and thawing are from the surface downwards and where permafrost is absent. Detailed continuous monitoring

of soil temperatures, frost heave, thaw consolidation, pore water pressures and downslope soil movement has allowed us to analyse the mass movement processes associated with soil freezing and thawing. An instrument package was developed for this purpose during full-scale laboratory simulation studies (Harris *et al.*, 1996), and an equivalent weather-proofed version was installed on a prominent solifluction lobe at Steinhøi in August 2001 (see Harris *et al.*, 2007, for details). A lightning strike in November 2001 caused instrument failure which was not repaired until 11 July 2002, and therefore data

* Correspondence to: Charles Harris, School of Earth Ocean and Planetary Sciences, Cardiff University, Cardiff CF10 3YE, UK. E-mail: harrisc@cardiff.ac.uk

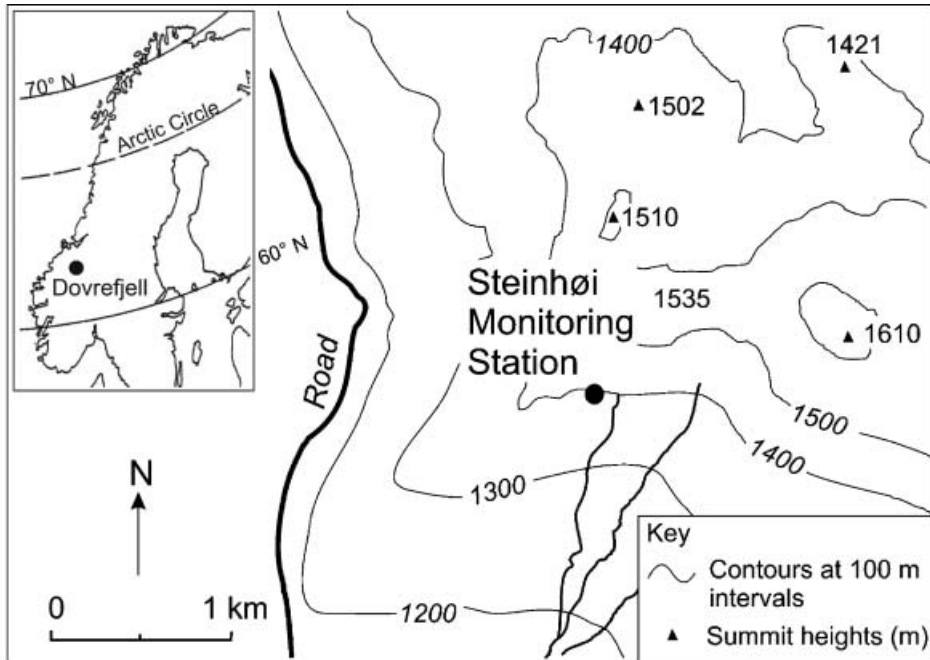


Figure 1 Location of the Steinhøi solifluction monitoring station.

only from the four year period from summer 2002 to summer 2006 are presented. The study is focused on processes rather than regional soil displacement rates. Given the range of surface gradients, snow conditions, drainage, etc., within the Steinhøi area, coupled with annual climatic variability, it is likely that rates of solifluction are spatially and temporally highly variable (see for instance, Washburn, 1999).

Although Andersson (1906) did not exclude non-periglacial environments in his original definition, the term solifluction has been widely used to describe slow periglacial mass movement caused by frost creep and gelifluction (e.g. Ballantyne and Harris, 1994; French, 2007; Matsuoka, 1998, 2001). Gelifluction and frost creep apparently operate in tandem, since both result directly from frost heave and thaw settlement. Where freezing and thawing are shallow and of short duration, creep movements dominate (e.g. Matsuoka, 2005), while gelifluction occurs during seasonal thawing of ice-rich soil (Washburn, 1967; Harris and Davies, 2000; Harris, 2007; Matsuoka, 2001). Recent laboratory studies have shown that gelifluction is best considered as elasto-plastic deformation that might be described as accelerated pre-failure creep rather than viscous flow (Harris *et al.*, 2003).

The role of high soil moisture content in promoting gelifluction has been emphasised in many field studies (e.g. Benedict, 1970; Washburn, 1979; Harris, 1981; Jaesche *et al.*, 2003; Kinnard and Lewkowicz, 2005) and several authors have reported moisture contents close to the Liquid Limit (e.g. Washburn, 1967; Smith, 1988; Kinnard and Lewkowicz, 2005). During laboratory simulations Harris *et al.* (1995, 1997, 2003, 2008) demonstrated very low shear strengths that persisted for only short periods immediately behind the thaw front when void ratios were high. Subsequent thaw consolidation rapidly lowered both void ratio and moisture content, and led to a rapid increase in soil strength. The mobilised frictional strength of these thawing ice-rich soils was largely a function of pore water pressure. High pore pressures and low effective stress values were recorded in the laboratory experiments for short periods (often only a few hours) immediately behind the thaw front.

Continuous monitoring in the Alps allowed Jaesche *et al.* (2003) to observe soil movements that lasted several days at given depths in a thawing soil, while Kinnard and Lewkowicz (2005) in southwest Yukon observed repeated discrete periods of displacement rather than slow incremental strains. Similarly,

Matsumoto and Ishikawa (2002) demonstrated that, on a gelifluction lobe in Sweden, soil movement was concentrated in two periods when ice-rich parts of the soil profile, firstly near the surface and secondly at a depth of around 20 cm, were in the process of thawing.

The aim of the present paper is to describe continuous field data collected from a slope where solifluction processes are active, in order that the influence of soil thermal conditions, frost heave/thaw settlement and hydraulic conditions may be explored.

SITE DESCRIPTION

The site lies above the treeline on the southern flanks of Steinhøi (Figure 1). It consists of a well-developed turf-banked solifluction lobe with a tread length of approximately 30 m and riser height around 1.5 m. (Figure 2). Turf-banked lobes are widespread across this slope. Bedrock comprises grey Proterozoic and Cambrian phyllite, biotite-phyllite and shale and forms part of the early Ordovician Gula-nappe (Geological Survey of Norway, 2002). The area is

mantled by Weichselian till with clasts up to boulder size set in a frost-susceptible matrix of silt and fine sand. Solifluction processes have reworked the till, and excavation during installation of instrumentation some 15 m upslope from the lobe front revealed 1–1.2 m of reworked till overlying bedrock and containing thin organic layers that likely extend from the lobe front and represent palaeo-surfaces buried by frontal advance (e.g. Matthews *et al.*, 1986, 2005).

Soil grain size distribution was measured from five samples collected at 10 cm depth intervals to a maximum depth of 60 cm. Clay contents were less than 4% except for the sample from 50–60 cm which showed 13%. Silt contents ranged from 16% to 38%. Occasional large clasts were not included in grain-size determinations. The soil has low plasticity (Plasticity Index 5%) with Plastic Limit 27% and Liquid Limit 32%.

The nearest meteorological station at Fokstugu (972 m), on Dovrefjell, has a mean annual air temperature of -0.1°C (1961–90) and mean annual precipitation of 435 mm. Hourly air temperatures



Figure 2 The Steinhøi monitored solifluction lobe showing the frost heave frame, with the LVDT fixed base triangle in the foreground and logger box and solar panel in the background. The apex of the LVDT triangle is attached to a footplate embedded in the ground surface (see Harris *et al.*, 2007, for details). Thermistors measuring air temperatures are shielded with white plastic tubing and attached to the solar panel pole. The station is fenced against large animals.

measured 2 m above the ground surface at Steinhøi during 2003, 2004 and 2005 show annual means of -0.1°C , -0.8°C and -0.1°C , but mean ground surface temperatures were more than 2°C higher, due largely to the insulating effect of winter snow. Storms are common in winter, accompanied by strong winds, and redistribution of snow by deflation leads to considerable spatial variation in snow thickness.

INSTRUMENTATION

Instrumentation was designed to monitor three key elements: ground surface movements (frost heave, thaw settlement and downslope solifluction), ground and air temperatures, and pore water pressures. In addition, profiles of soil movement (the distribution of shear strain with depth) were measured over a four year period (2002–06).

Ground and Air Temperatures

Stainless steel thermistor probes supplied by Campbell Scientific Ltd formed a vertical array above and below the ground surface. Thermistors were installed at the ground surface and at 10 cm intervals to a depth

of 80 cm (Figure 3). Thermistors, shielded by 2 cm diameter white plastic tubing, were also mounted on the pole supporting the solar panel at heights of 50, 100 and 200 cm. Temperature measurement errors are estimated to be up to $\pm 0.4^{\circ}\text{C}$. The 10 cm thermistor proved unreliable, and data from this depth were not used.

Pore Water Pressure

A vertical array of five Druck PDCR81 pore pressure transducers was installed at 10 cm depth intervals between 20 and 60 cm. Transducers were filled with low viscosity silicon oil and had a range of 350 mb, combined non-linearity and hysteresis of $\pm 0.2\%$ and thermal sensitivity of 0.2% of reading per $^{\circ}\text{C}$.

Ground Surface Movements

Continuous monitoring of ground surface movements requires a stable reference datum, though Berthling *et al.* (2000) reported three-dimensional target movements measured using carrier-phase Differential Global Positioning System (DGPS). In the present study, a stable frame was constructed from steel scaffolding poles of external diameter 5 cm. The frame

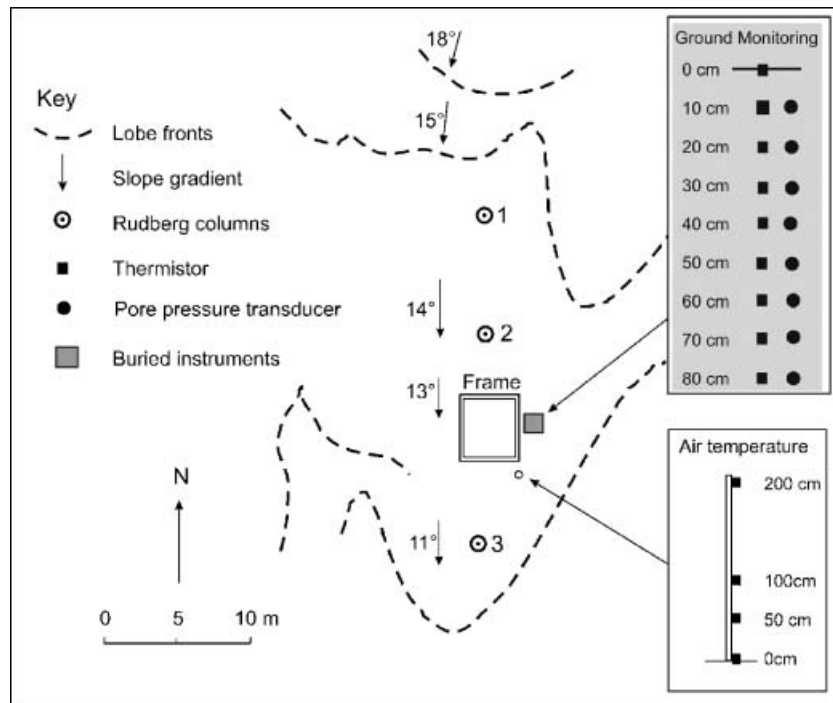


Figure 3 Site plan showing location of instrumentation.

dimensions were 2 m × 2.2 m × 0.95 m. Diagonal side struts increased rigidity. The supporting legs were vertical, though subsequent laboratory physical modelling has shown the development of significant downslope bending stresses as a result of winter frost heave perpendicular to the surface (Ripley, 2004). Frame legs extended to bedrock at a depth of 1–1.2 m and the lowermost 0.5 m was embedded in concrete. The remaining buried section was greased and sheathed in telescopic plastic tubing to isolate it from adjacent frost heaving soil.

Soil surface motion was measured using a pair of waterproof captive guided armature DC/DC linear variable differential transformers (LVDTs) (350 mm range). The configuration of LVDTs allowed measurement of soil displacement with an accuracy of ±1.5 mm over the operating temperature range. Two LVDTs were mounted via spherical end bearings on a central scaffolding pole supported by the frame, running parallel to the ground surface along the slope fall line and extending upslope from the frame (Figure 2). LVDTs formed a fixed base triangle at the apex of which was an 8 cm × 5 cm stainless steel footplate embedded in the soil surface. Frost heave, thaw settlement and downslope displacements of the ground surface were detected by changes in length of the LVDTs and hence geometry of the fixed base triangle (see Harris *et al.*, 2007, for details).

The horizontal cross members supporting the LVDT beam were instrumented with pairs of strain gauges glued to the steel poles with epoxy resin. Although not directly calibrated, these indicated periods when snow loading caused slight bending and therefore lowering the LVDT support beam relative to the ground surface, registering as apparent heave in the LVDT readings. Such loading was evident in the winter of 2004–05, and LVDT data from that winter are not presented here. In other years no significant deflection of the beams was apparent.

Data Acquisition

All data were recorded at hourly intervals via Campbell Scientific CR23X loggers with a 16/32 channel multiplexer. The logger was powered by a 12 V heavy-duty car battery charged with an 18 W solar panel (Figure 2). All cabling between sensors and logger was either buried, or protected from damage by animals by plastic tubing.

Profiles of Soil Movement: Rudberg Columns

Three Rudberg columns were installed in a downslope transect (Figure 3). Columns comprised 2 cm long

sections of plastic tubing of external diameter 2 cm. Sections were threaded over a steel rod slightly smaller in diameter than the internal diameter of the tubing to form column lengths of around 75 cm, and these were pushed into an auger hole perpendicular to the ground surface. The steel rod was then withdrawn, leaving column sections free to move with the soil. Columns were installed in July 2001 and re-excavated in August 2005, indicating the accumulated movement over a four year period.

RESULTS

Thermal Regime

Air Temperatures and Inferred Snow Depths.

Figure 4 shows temperatures recorded at 200, 100, 50 and 0 cm above the ground surface from 2002 to 2006. Minimum temperatures of around -20°C were recorded, but only January was free of above zero air temperatures in each of the four years. The temperature record shows that during winter 2002–03, the thermistor probe located 50 cm above the ground surface lay above the snow (time bar (a), Figure 4) since its temperature time series was virtually identical to those at 100 and 200 cm. In 2003–04 temperature fluctuations in the 50 cm thermistor were significantly dampened from early February until late April (time bar (b), Figure 4), indicating that snow depth was greater than 50 cm but less than 100 cm in this period. In 2004–05 snow depth was greater than 50 cm from mid January to early June (time bar (c), Figure 4) and greater than 100 cm through much of April and May (time bar (d), Figure 4). During this period of thick snow cover the frame suffered significant snow loading, and LVDT data could not be used to determine ground surface movements. Winter 2005–06 was characterised by repeated short-term surface freeze-thaw cycles in the autumn (Table 1), (time bar (e), Figure 4) with final winter surface freezing not commencing until 7 November 2005, some three to four weeks later than in the previous three years. Snow thickness was less than 50 cm until mid March but from mid March until the beginning of May, depths were between 50 and 100 cm (time bar (f), Figure 4).

Soil Temperatures.

The near-surface ground thermal regime is strongly influenced by snow conditions, with the relatively snow-poor winter of 2002–03 showing greatest frost penetration (38 cm), compared with around 30 cm in 2003–04 and 2004–05, and slightly more than 30 cm

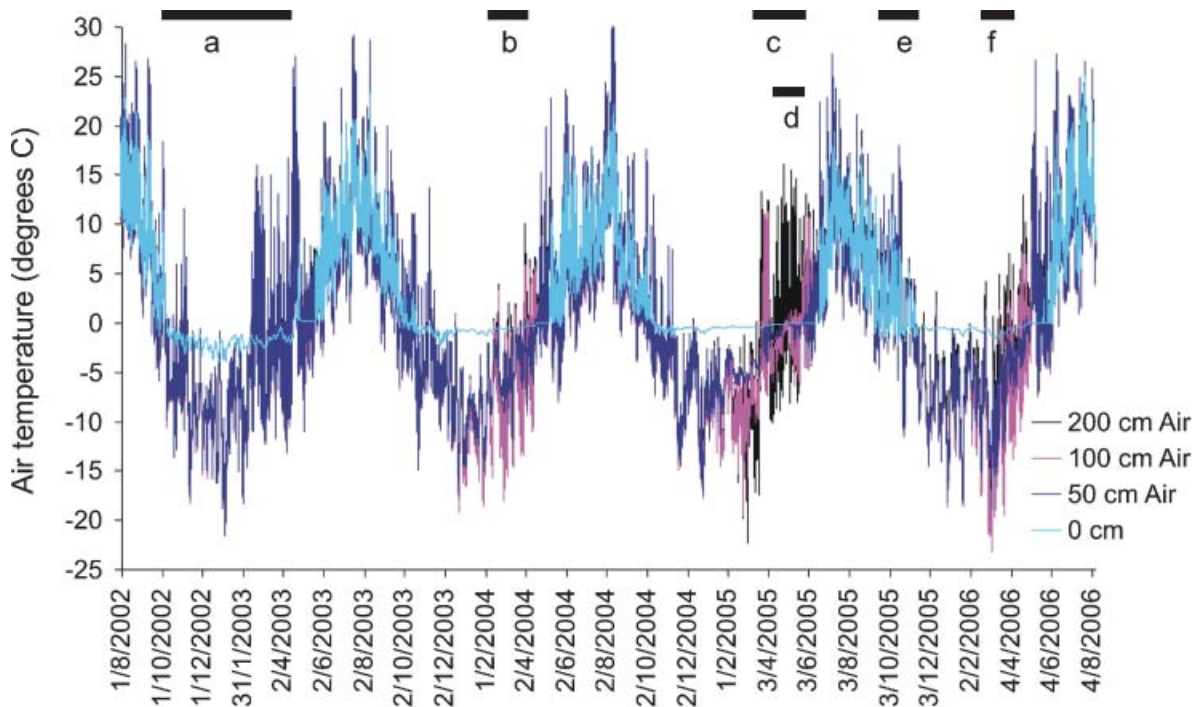


Figure 4 Air and ground surface temperatures from August 2002 to July 2006. Time bars are referred to in the text.

in 2005–06 (Figure 5). Ground surface temperatures were lowest in 2002–03, with minimum recorded temperature -4°C in December (Figure 5).

Thermistors located below the depth of seasonal frost penetration recorded strong cooling in late winter/early spring (indicated by time bars (a)–(d) in Figure 6). Cooling was caused by heat advection as cold meltwater from higher upslope flowed beneath the frozen surface layer. The effect was greatest in the snow-rich winter of 2004–05 (time bar (c), Figure 6), and least in the snow-poor winter of 2002–03 (time bar (a), Figure 6).

Pore Water Pressures

Figure 7 presents pore pressures recorded at 20, 40 and 50 cm depths, together with soil temperatures. The transducers at 40 and 50 cm depths remained unfrozen throughout the period and showed considerable

variation in pore pressure (Figure 7c and 7d). Pressures were low but fluctuating through the winter, and increased very rapidly during spring as air temperatures rose and the nival thaw commenced, confirming that snowmelt was flowing beneath the frozen near-surface soil layers. In 2004 this seepage began at 40 cm depth some three weeks before the soil surface temperatures rose above zero, and in 2005 and 2006 some four weeks before surface thaw commenced. Pore pressures were in excess of hydrostatic, particularly during the period when the still-frozen near-surface soil formed a confining layer. At 40 cm, pore pressures reached a maximum of 96 cm of water (9.8 kPa) for a few hours in late April 2004 (Figure 7c), which is in excess of geostatic (meaning the self weight of the overburden would have been supported by pore pressures). However, at that time the frozen ground above was sufficiently rigid to prevent shallow landsliding. By the time the surface layer had thawed, pore pressures at 40

Table 1 Summary of time periods with frozen ground.

	2002–03	2003–04	2004–05	2005–06
Autumn frost cycles at 0 cm	2	2	0	6
Winter ground freezing begins	07/10/02	19/10/03	11/10/04	7/11/05
Completion of ground ice melt	06/06/03	26/05/04	04/07/05	12/06/06

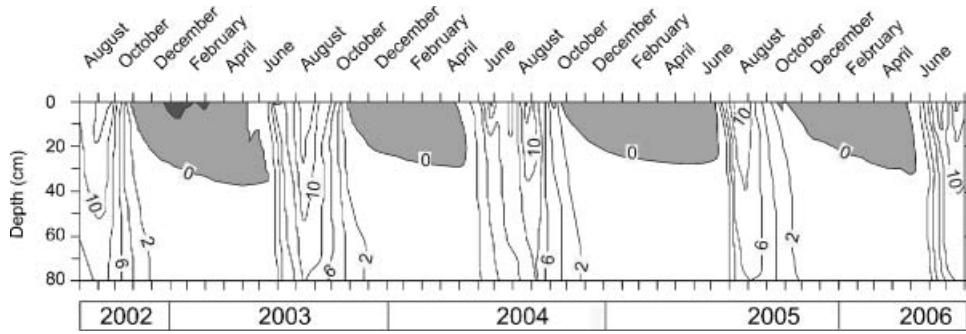


Figure 5 Isotherms in degrees Celsius showing frost penetration over four winters, from 2002 to 2006. Shaded areas are below zero Celsius.

and 50 cm depth were only slightly in excess of hydrostatic and insufficient to cause instability. At 50 cm, pore pressures were slightly lower, rising to above 60 cm water (5.9 kPa) in spring 2004 and 2005, and to a maximum of 45 cm water (4.4 kPa) in spring 2006, and remaining high for a further three to four weeks after soil thawing was complete.

The fact that pore pressures at 40 cm were higher than at 50 cm and began to rise before those at 50 cm

may indicate a zone of preferential seepage, probably relating to higher permeability at this depth. The rapid fall in pressures in late spring or early summer was synchronous at 40 and 50 cm in all three years, reflecting the final clearance of much of the snow upslope from the site and therefore the loss of melt-water seepage. Temporal periodicity in pore pressure fluctuations was generally longer than diurnal (though a weak diurnal signal is also detectable) prior to

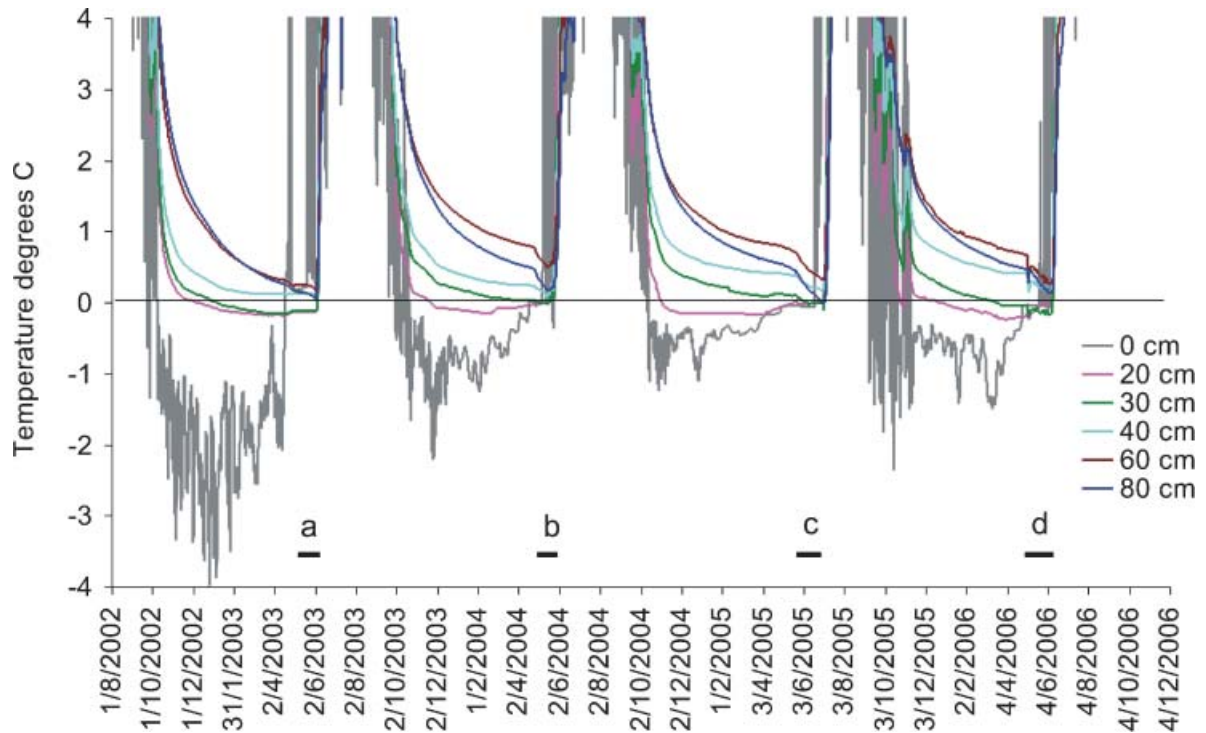


Figure 6 Soil temperatures 2002–06. Time bars indicate periods of late winter/early spring ground cooling caused by meltwater flow beneath the frozen near-surface layers.

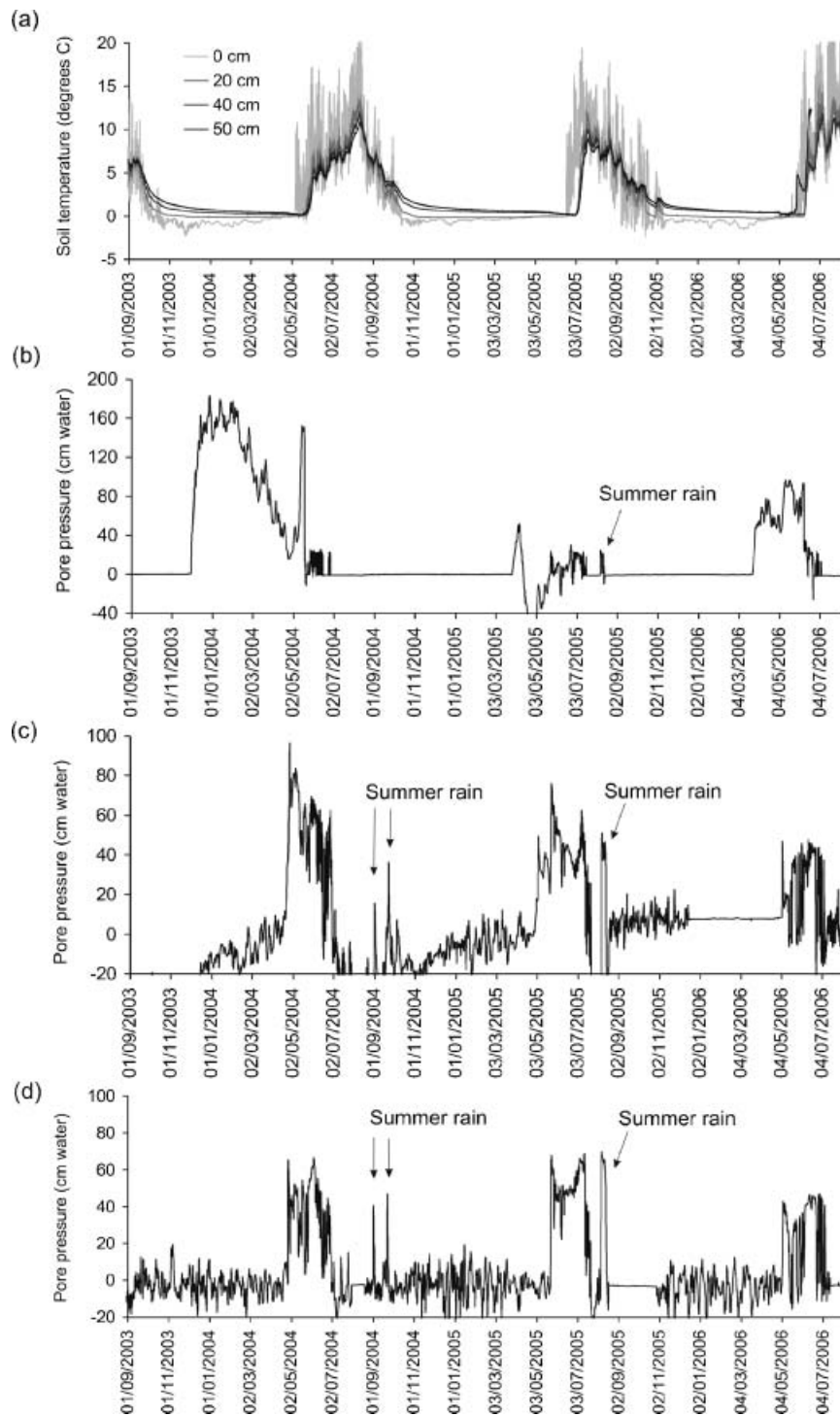


Figure 7 Time series of soil temperatures and pore water pressure. (a) Soil temperatures. (b) Pore water pressures recorded at 20 cm depth. Pore pressure response to the summer rainfall event in August 2005 is labelled. (c) Soil temperatures and pore water pressures recorded at 40 cm depth. Pore pressure responses to summer rainfall events are labelled. (d) Pore water pressures recorded at 50 cm depth. Pore pressure responses to summer rainfall events are labelled.

clearance of the frozen surface layer, but subsequently became markedly diurnal (Figure 8). Occasional influxes of surface water associated with rainfall events were registered through the summer periods when the soil was completely thawed (examples are labelled in Figure 7c and 7d).

At 20 cm depth, the pore pressure transducer response was related closely to phase changes within the soil in winter and spring, though the signal from 2005 is less clear than in the previous and succeeding years (Figure 7b). All transducers were recalibrated and re-installed in July 2005. During winter 2003–04 the minimum temperature recorded at 20 cm depth was -0.2°C , and sub zero temperatures persisted from early December to late May. It should be noted that the precision of temperature measurements is insufficient to discriminate very small temperature changes, but evidence of frost heave and measurement of heaving pressures provide clear evidence of freezing at this depth. The formation of segregation ice led to significant ice pressures in winter 2003–04 (Figure 7b). These declined slowly as heaving rates decreased. Surface thaw began on 17 April 2004, and surface temperatures rose rapidly on 7 May. The thaw front reached a depth of 20 cm on 18 May. Prior to this, meltwater from the surface apparently migrated downwards into the underlying still-frozen soil (along the thermal gradient) during thaw penetration and caused renewed ice segregation at 20 cm depth during

the first two weeks of May 2004 (Figures 7b and 8), when ice pressures increased rapidly and renewed frost heave was registered by the LVDTs (see below). This is probably equivalent to Mackay's observation of 'summer heave' above permafrost in the Canadian arctic (Mackay, 1983), though in this seasonally frozen context, resulting soil ice soon thawed again. Ice pressures fell rapidly as thawing at 20 cm began. Thawing was complete on 26 May 2004, when pore pressures at 20 cm rose to slightly in excess of hydrostatic (equivalent to 23.6 cm water or 2.3 kPa), and fluctuated around this level for the next 20 days. Thus the soil remained saturated at 20 cm depth for around three weeks after thawing in 2004, corresponding to the period of high pore pressures recorded at 40 cm depth.

The winter of 2004–05 was snow-rich and initiation of ground thawing was delayed until late June. Consistent ice pressures were not recorded at 20 cm (Figure 7b), but immediately following soil thaw, pore pressures rose to a maximum value of 28.5 cm water (27.9 kPa) and remained elevated for three weeks. The rainstorm event in the second week of August 2005 was clearly registered, with pore pressures of 20.8 cm water (labelled in Figure 7b), equivalent to a water table at or slightly above the ground surface.

In winter 2005–06, winter ice segregation pressures were again registered at 20 cm, though not until

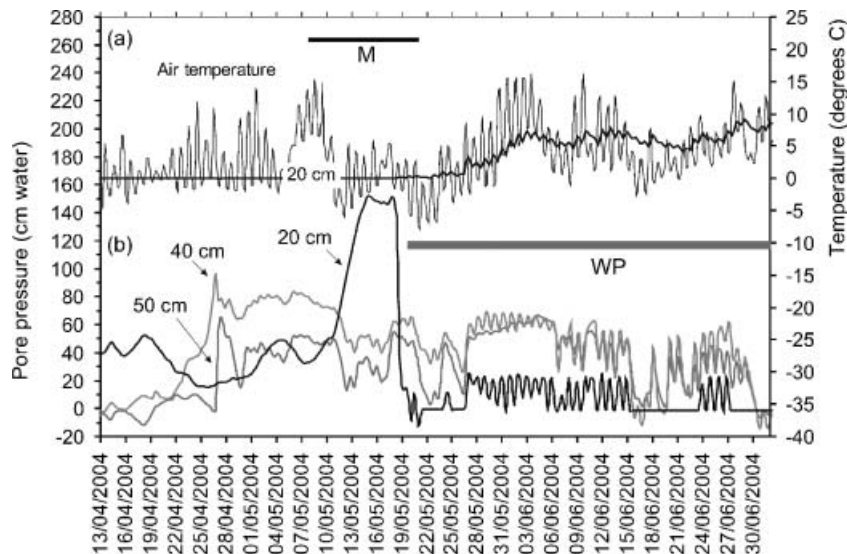


Figure 8 Air temperature, soil temperature at 20 cm and pore pressures, spring 2004. The bar labelled WP indicates the period when pore water pressures (as opposed to ice pressure) were recorded at 20 cm depth. The bar labelled M shows the period when soil surface downslope displacements took place.

March. These persisted until initiation of thawing at this depth, on 10 June 2006, when ice pressures fell rapidly and soil temperatures rose sharply above zero (Figure 7b). A small peak in ice pressures immediately before thawing probably corresponded to ice segregation due to downward migrating water, and this was registered by the LVDTs as slight surface frost heave (see below). Following thaw, pore pressures at 20 cm were again in excess of hydrostatic, decreasing over a period of some two weeks from an initial high of around 33 cm water (3.4 kPa).

Frost Heave, Thaw Settlement and Downslope Surface Displacements

Data were collected for the period from August 2002 to August 2006, but thick snow cover in winter 2004–05 caused deformation of the beam supporting the LVDTs so that apart from the early heaving phase prior to the commencement of snow loading, data for this year cannot be interpreted. The record shows that both frame and LVDTs were also disturbed in July 2005, possibly by a large animal. The system was

repaired in August 2005, so that data for 2005–06 are re-zeroed and presented separately.

Movement of the LVDT footplate was resolved into displacements perpendicular to the ground surface (heave and settlement) and parallel to the ground surface (downslope movement and retrograde movement).

Phases of Heave-settlement through Time.

Five distinct periods may be identified in the record for 2002–03 and 2003–04, labelled (a)–(e) in Figure 9. In the summer (period (a)), soils were relatively dry and the ground largely stable. Period (b), in autumn and winter, showed frost heave and apparent upslope movement of the footplate during ground freezing. Heaving was initially rapid, but slowed later in the winter. Apparent upslope movement of the footplate is ascribed to small downslope movements of the LVDT support bar resulting from lateral stresses on the vertical frame legs caused by frost heave perpendicular to the ground surface (see Harris *et al.*, 2007, for details). The first sign of thaw settlement marked the start of period (c) when ground surface temperatures

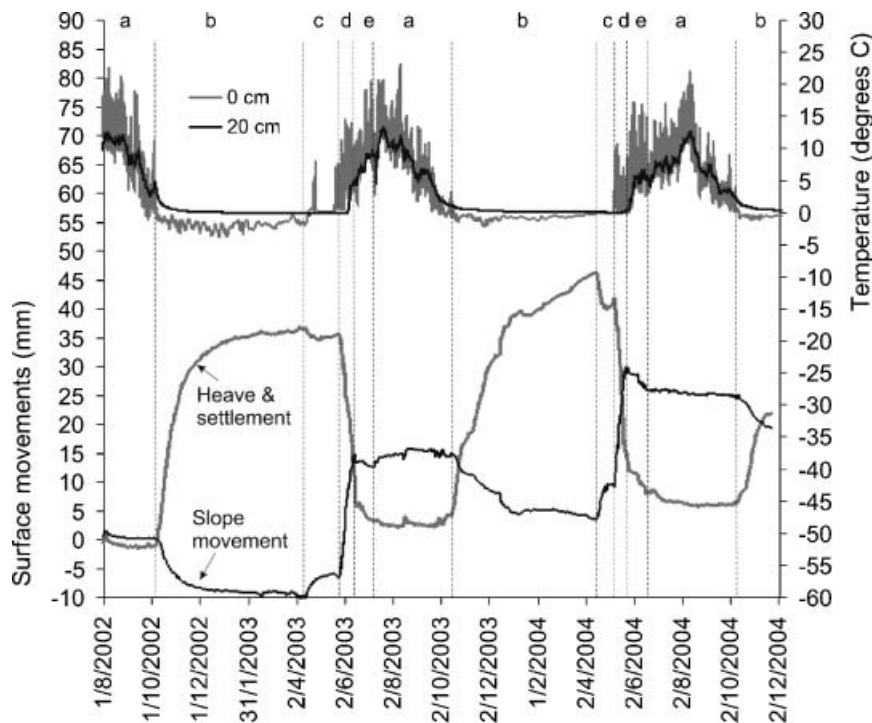


Figure 9 Heave, settlement and downslope/upslope soil movement (left axis) plotted with temperatures (right axis) August 2002–July 2004. Upper graph shows temperatures at the surface and 20 cm. Lower graph shows LVDT movement data with grey line marking heave and resettlement and black line downslope (increasing values) and upslope (decreasing values) soil movements. See text for explanation of time periods labelled (a) to (e).

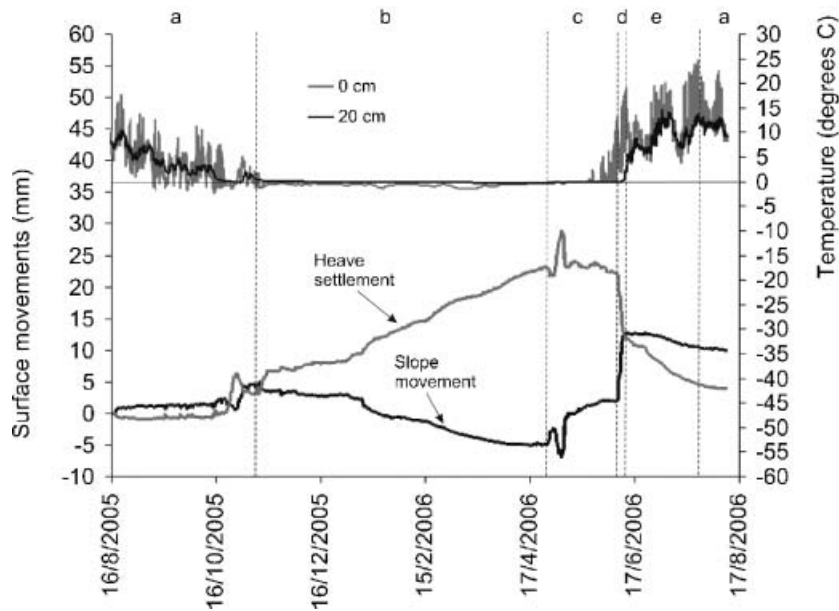


Figure 10 Phases of heave, settlement and downslope/upslope soil movement (left axis) plotted with temperatures (right axis), August 2005–August 2006. Upper graph shows temperatures at the ground surface and at 20 cm. Lower graph shows LVDT movement data. Grey line — heave and resettlement, black line — soil movements downslope (increasing values) and upslope (decreasing values). See text for explanation of time periods labelled (a) to (e).

were 0°C and thaw had begun. In all years, but particularly in 2004, initial thaw settlement and accompanying downslope surface movements in period (c) were interrupted by slight heaving towards the end of the period. This renewed heaving corresponded with a sharp increase in ice pressures at 20 cm, a few days before the thaw plane arrived (see above).

The establishment of a steeper thermal gradient in the thawing soil as ground surface temperatures rose, resulted in more rapid thaw penetration with associated thaw settlement and downslope surface movements (period (d)) and corresponded with the main phase of ground thawing. Period (d) lasted 19 days (26 May–14 June) in 2003 and 13 days (8–21 May) in 2004, and both settlement and downslope surface displacements were rapid. The final stage in the annual cycle (period (e)) followed clearance of ground ice, and corresponded to a

decrease in the rate of settlement and the development of retrograde (upslope) movement of the soil surface relative to the frame. The LVDT mounting beam was stable at this stage since there were no longer any lateral heaving pressures on the frame legs. The upslope surface ground movement represented retrograde movement as the soil dried (e.g. Washburn, 1967; Harris and Davies, 2000).

Figure 10 shows a similar pattern of frost heave, thaw settlement and downslope surface movements in 2005–06 compared with the earlier years, though with some variations. At the end of period (a), in the last week of October 2005, a cycle of surface freezing and thawing caused initial heave and thaw settlement before the main winter phase of soil freezing commenced (period (b), Figure 10). Frost heaving through the winter was progressive, but was less than in 2002–03 or 2003–04 (Table 2). The soil surface temperature rose to 0°C on 1 May 2006, and immediate slight

Table 2 Frost heave, thaw settlement and downslope surface displacements, 2002–03, 2003–04 and 2005–06.

	2002–03	2003–04	2005–06
Net frost heave (mm)	38	44	29
Net thaw settlement (mm)	34	40	25
Net surface downslope movement (mm)	13	13	9

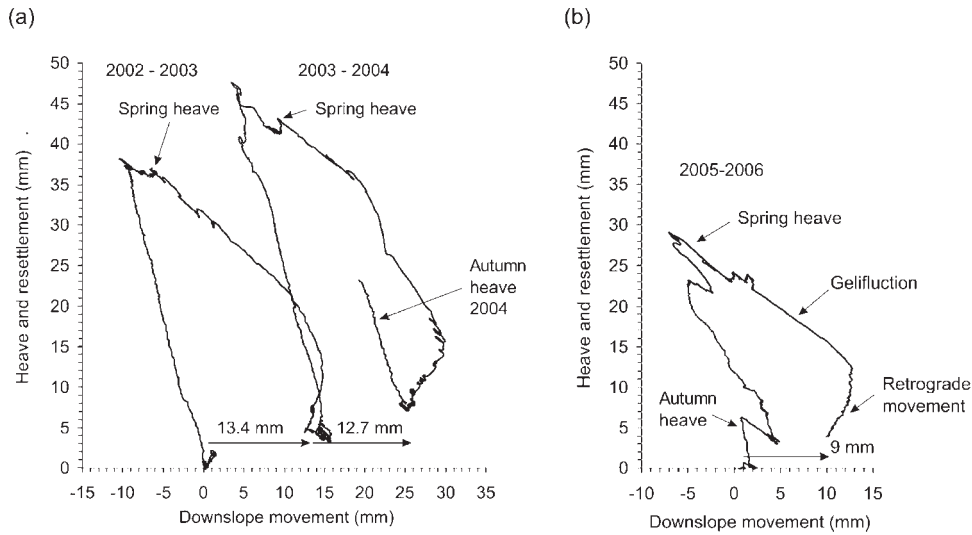


Figure 11 Vectors of surface movement: (a) 2002–03 and 2003–04; (b) 2005–06.

thaw settlement was registered (initial part of period (c)). This was followed by heave amounting to some 7 mm, then further and much greater thaw settlement, with the whole cycle being complete by 8 May. No ice pressures were registered at 20 cm during the thaw phase, so it is likely that thaw-phase heaving was due to ice segregation at shallower depths for a period of two or three days following initiation of surface thaw. Despite surface temperatures rising above 0°C at the end of May, the onset of rapid thaw settlement and downslope displacement (period (d)) was delayed until 7 June, movement continuing for only four days until 10 June. Period (d) was followed, as previously, by a phase of further settlement and retrograde movement (period (e)) at the end of the heave-settlement cycle.

Vectors of Soil Surface Movement.

Combining heave and downslope displacement data provides a vector of soil surface movement through each annual cycle (Figure 11). The apparent upslope movement during heave caused by deflection of the frame is clear in all three years. The short periods of renewed ice segregation caused by refreezing of percolating meltwater following initiation of surface thaw are indicated in Figure 11. These were followed by a phase of gelifluction during thaw consolidation, and then a period of retrograde movement associated with soil drying and consolidation following final thaw. In each year the LVDT footplate embedded in the ground surface moved downslope, but the ground

surface also apparently rose by a few millimetres each year relative to the frame. This apparent rise was due to a progressive decrease in the ground surface slope, from approximately 14° to 12°, and the fact that the slope of the frame beam supporting the LVDT triangle was slightly greater than that of the underlying ground, so that as the footplate moved downslope, the height difference between the support beam and ground surface decreased slightly. Net heave and downslope displacement data are presented in Table 2. Although heave is apparently the dominant factor in the amount of soil movement, greater retrograde movement in 2004 resulted in a smaller net displacement than in 2003, despite greater frost heave.

Profiles of Soil Movement

Three Rudberg columns, located along the lobe axis, were excavated in summer 2006 (Figure 12) and revealed net soil movement profiles over a period of four years. Average annual surface displacement, the depth of displacement and the volumetric transport rate increased significantly from the rear of the lobe tread to the frontal zone (Table 3). In the higher part of the lobe tread, soil displacements were detected to a depth of 22 cm in profile 1, while in the mid-tread location, just upslope of the frame, the depth of movement was 43 cm (profile 2), and in the lowermost measured displacement profile, below the monitoring

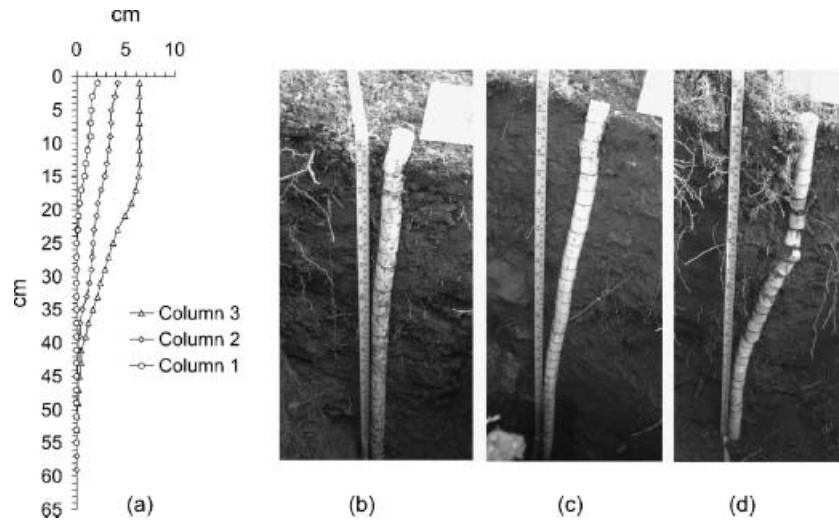


Figure 12 Soil displacement profiles August 2001–August 2005. (a) Measured profiles; (b) profile 1 (rear of lobe tread); (c) profile 2 (immediately above monitoring frame); (d) profile 3 (below monitoring frame in lobe frontal zone).

Table 3 Soil displacement measured by Rudberg columns installed in August 2001 and excavated in August 2005.

	Profile 1	Profile 2	Profile 3
Average surface movement rate (cm yr^{-1})	0.5	1.0	1.6
Average volumetric transport rate ($\text{cm}^3 \text{cm}^{-1} \text{yr}^{-1}$)	6	22	46
Maximum depth of soil movement (cm)	22	43	50

frame, this depth of displacement reached 50 cm. Movement rates decreased with depth in profiles 1 and 2, but in profile 3 a convexo-concave profile was observed, similar to that described by Matsuoka (2001) as typical of solifluction profiles caused by one-sided soil freezing and thawing. Typical rates of soil transport by solifluction are quoted by Matsuoka (2001) as being in the range $20\text{--}50 \text{ cm}^3 \text{ cm}^{-1} \text{ yr}^{-1}$, which corresponds well with observations here.

DISCUSSION

Mechanisms of Movement

Despite the extended periods of soil saturation following ground thawing and short-term periods of raised pore pressures during summer rainstorms, downslope soil displacements were recorded only during the period of thaw consolidation. Later surface settlement was associated with retrograde movement

(Figure 11). Once thawing was complete, downslope displacements in 2004 and 2006 ceased, but in 2003 settlement and downslope movement continued for a further eight days. Thus the period of downslope surface movement was relatively short, lasting approximately 19 days in 2003, 13 days in 2004 and only four days in 2006. Measured average rates of movement during these periods were 1.1 mm per day in 2003, 1.5 mm per day in 2004 and 2.5 mm per day in 2006.

Washburn (1967) defined the term potential frost creep as the maximum creep that would be anticipated arising from frost heave perpendicular to the ground surface, followed by vertical settlement during soil thaw, under the influence of gravity. Potential frost creep is therefore the product of total heave and the tangent of the slope angle. It is generally considered that actual creep movements are less than this potential value due to the effects of cohesion within the moist soil mass. Figure 13 presents an analysis of the main thaw settlement phases in each of the three

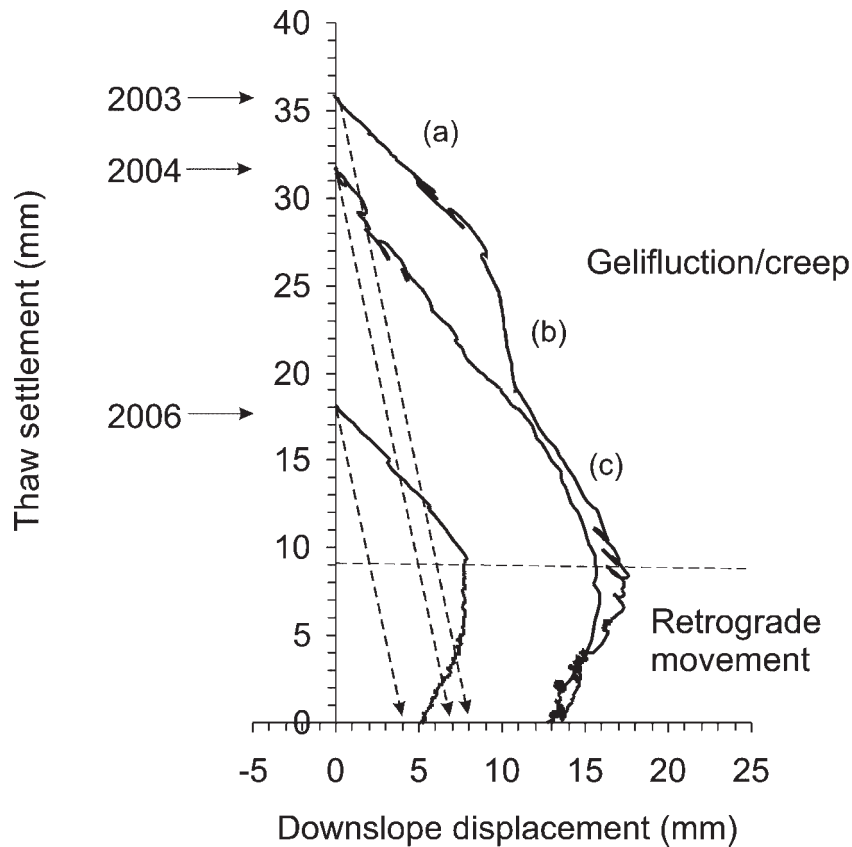


Figure 13 Vectors of surface movement during the main periods of thaw settlement in 2003, 2004 and 2006. Dashed arrows show the trajectories of the soil surface if thaw settlement were vertical, that is, the potential frost creep trajectories. For labelling of the 2003 vector, see text.

years 2003, 2004 and 2006. It is assumed that the slight downslope distortion of the frost heave frame (manifest in apparent upslope component of frost heave in the observed surface vectors — see Figure 11) was progressively recovered through this period of thaw settlement, and that the frame returned to its pre-frozen geometry by the end of the thaw cycle. This has been accounted for in Figure 13 by distributing the additional apparent ground surface movement due to frame recovery evenly through the thaw period, and subtracting this from the raw data. Potential frost creep accounted for 66% of the net surface movement (including the retrograde movement) in 2003, 53% in 2004 and 76% in 2006. As Figure 13 demonstrates, it is, in reality, impossible to separate creep movements from gelifluction.

Total downslope movements in 2003 and 2004 shown in Figure 13 are identical to those determined for the full vectors in Figure 11a (i.e. 13.4 and

12.7 mm). However, in 2006 the downslope displacement arising from the main phase of thaw settlement totalled only 5.2 mm, compared with an annual measured total of 9 mm from the vector in Figure 11b. The discrepancy is due to an additional increment of movement resulting from the short period of soil freezing and thawing in the autumn of 2005 which lasted from 22 October to 10 November, prior to the main winter cycle of freezing.

Two main phases of thaw settlement are recognised: firstly, settlement associated with gelifluction/creep, and secondly a succeeding period of settlement associated with retrograde movement. The gelifluction/creep phase in 2003 was subdivided into two periods of more rapid downslope movement labelled (a) and (c) in Figure 13, and a period with much less downslope movement, labelled (b). There appears to be some consistency in the ratio of downslope surface displacement to thaw settlement during the gelifluction/creep stage over the

monitored three years. With the exception of period (b) (Figure 13) in 2003, when it was 0.13, the ratios in 2003 were 1.05 and 0.74 (periods (a) and (b)), respectively. In 2004 the ratio was 0.8 and in 2006 it was 1.04. The equivalent ratio for vertical soil resettlement (maximum potential frost creep) is around 0.23 (the tangent of 13°).

Harris *et al.* (1997) demonstrated a consistent displacement-settlement ratio over a number of freeze-thaw cycles of around 1.5 for a silt-rich test soil used in full-scale laboratory simulations on a slope with a gradient of 12° (similar to the gradient here). Thus, it appears that the laboratory soil had a higher susceptibility to solifluction than the present Steinhøi field soil.

Pore Water Pressures

Simulation experiments, both at full-scale (Harris *et al.*, 1997) and at reduced scale in the geotechnical centrifuge (Harris *et al.*, 2003, 2008), have demonstrated the importance of low soil shear strengths during gelifluction. High pore pressures have been recorded during thaw consolidation when both soil void ratios and moisture contents are initially high, but decreasing. Here we recorded maximum pore pressures of between 3.4 kPa and 2.6 kPa during thaw consolidation at 20 cm depth, exactly within the range of values recorded at similar depths in the full-scale and centrifuge simulation experiments referred to above. At some point during consolidation, void ratios and moisture contents reach critical values at which the soil becomes too stiff to undergo further shear strain under self weight stresses. Gelifluction then ceases, though volume strain continues due to soil drying. At Steinhøi, post-thaw pore water pressures at 20 cm were modulated strongly by high pore pressures associated with meltwater seepage at 40 cm depth, and therefore the thaw consolidation signal is less clear than might otherwise have been the case.

CONCLUSIONS

This paper, like several recent contributions to our understanding of periglacial solifluction processes (e.g. Kinnard and Lewkowicz, 2005; Jaesche *et al.*, 2003; Matsumoto and Ishikawa, 2002; Matsumoto *et al.*, 2001; Matsuoka, 1994, 2005), has emphasised the importance of continuous monitoring of site

variables. Through this approach we have explored the relationships between soil movements and a range of factors including ground temperatures, frost heave, thaw settlement and soil moisture conditions, particularly pore pressures.

Observed rates of solifluction on the monitored solifluction lobe at Steinhøi, Norway, were lowest near the rear of the lobe (0.5 cm per year over a four year period, equivalent to $6 \text{ cm}^3 \text{ cm}^{-1} \text{ yr}^{-1}$ volumetric soil transport) and highest near the front (1.6 cm yr^{-1} , equivalent to $46 \text{ cm}^3 \text{ cm}^{-1} \text{ yr}^{-1}$ volumetric soil transport). Continuous monitoring has shown that following initiation of surface thaw, downward percolation of meltwater into the still-frozen soil below caused renewed ice segregation and slight frost heave. Subsequently, soil thawing was associated with settlement and downslope displacements, the main period of solifluction lasting 19 days in 2003, 13 days in 2004 and only four days in 2006. Thus, it is concluded that soil shear strain occurred immediately behind the advancing thaw front as a result of high pore pressures generated as water-filled voids were closed during thaw consolidation. At 20 cm, however, recorded pore pressures were also affected by meltwater seepage at greater depths.

Frost penetration was shown to be highly sensitive to snow depth and ranged from 38 cm in 2002–03 when snow depth was less than 50 cm to around 30 cm during 2004–05 when maximum snow depths exceeded 100 cm. Large spatial variation in frost penetration depths in response to variable snow thickness is also suggested by meltwater seepage beneath the seasonally frozen surface layer of the monitored solifluction lobe. It is assumed that snow arrived sufficiently early and was sufficiently deep to prevent ground freezing in certain accumulation hollows upslope from the monitored lobe, thus providing entry points for groundwater seepage beneath the seasonally frozen layer further downslope. In 2005–06, frost heave and thaw settlement were much less than in previous years, and since the ratio of surface gelifluction to thaw settlement was roughly constant in each year, the amount of gelifluction was also significantly lower. It is concluded that, as observed by Jaesche *et al.* (2003) in the Austrian Alps, spatial and temporal variability in snow cover probably plays the greatest role in determining frost penetration depths and frost heave totals, and therefore contributes significantly to spatial and temporal variability in downslope soil transport by gelifluction. Any future trends toward warmer winter temperatures or increased snow fall at this site would have the effect of reducing rates of gelifluction.

ACKNOWLEDGEMENTS

The authors wish to thank the following for their support in the field: Professor Johan Ludvig Sollid, James Smith, Rune Strand Ødegård, Karsten Vedel Johansen and Trond Eiken. The mountain supervisor in Follidal, Mr Odd Enget, gave permission for the installations at Steinhøi and helped with local transport. Funding for this research was provided by the British Engineering and Physical Sciences Research Council (EPSRC GR/T22964) and by Cardiff University. Logistical support from the University of Oslo and the Norwegian Meteorological Institute is gratefully acknowledged. Professor J.L. Sollid kindly allowed us to use the facilities of the Hjerkin field station. The comments of the anonymous reviewers on an earlier version of the paper are appreciated.

REFERENCES

- Andersson JG. 1906. Solifluction, a component of sub-aerial denudation. *Journal of Geology* **14**: 91–112.
- Ballantyne CK, Harris C. 1994. *The Periglaciation of Great Britain*. Cambridge University Press: Cambridge.
- Benedict JB. 1970. Downslope soil movement in a Colorado alpine region: rates, processes, and climatic significance. *Arctic and Alpine Research* **2**: 165–226.
- Berthling I, Eiken T, Sollid JL. 2000. Continuous measurements of solifluction using carrier-phase differential GPS. *Norsk Geografisk Tidsskrift-Norwegian Journal of Geography* **54**: 182–185.
- French HM. 2007. *The Periglacial Environment*, 3rd edn. John Wiley: Chichester.
- Geological Survey of Norway. 2002. Bedrock map Follidal 1519 II, Scale 1:50 000.
- Harris C. 1981. *Periglacial Mass Wasting: A Review of Research*. BGRG Research Monograph. Geo Books: Norwich.
- Harris C. 2007. Slope deposits and forms. In *Encyclopedia of Quaternary Science*, Elias SA (ed.). Elsevier: Amsterdam; 3, 2207–2216.
- Harris C, Davies MCR. 2000. Gelifluction: observations from large-scale laboratory simulations. *Arctic, Antarctic and Alpine Research* **32**(2): 202–207.
- Harris C, Davies MCR, Coutard J-P. 1995. Laboratory simulation of periglacial solifluction: significance of porewater pressure, moisture contents and undrained shear strength during thawing. *Permafrost and Periglacial Processes* **6**: 293–312.
- Harris C, Davies MCR, Coutard J-P. 1996. An experimental design for large-scale modelling of solifluction processes. *Earth Surface Processes and Landforms* **21**: 67–76.
- Harris C, Davies MCR, Coutard J-P. 1997. Rates and processes of periglacial solifluction: an experimental approach. *Earth Surface Processes and Landforms* **22**.
- Harris C, Davies MCR, Rea BR. 2003. Gelifluction: viscous flow or plastic creep? *Earth Surface Processes and Landforms* **28**: 1289–1301.
- Harris C, Luetschg MA, Davies MCR, Smith FW, Christiansen HH, Isaksen K. 2007. Field instrumentation for real-time monitoring of periglacial solifluction. *Permafrost and Periglacial Processes* **18**: 105–114. DOI: 10.1002/ppp.573
- Harris C, Smith JS, Davies MCR, Rea B. 2008. An investigation of periglacial slope stability in relation to soil properties based on physical modelling in the geotechnical centrifuge. *Geomorphology* **93**: 437–459. doi:10.1016/j.geomorph.2007.03.009.
- Jaesche P, Veit H, Huwe B. 2003. Snow cover and soil moisture controls on solifluction in an area of seasonal frost, Eastern Alps. *Permafrost and Periglacial Processes* **14**: 399–410. DOI: 10.1002/ppp.471
- Kinnard C, Lewkowicz AG. 2005. Movement, moisture and thermal conditions at a turf-banked solifluction lobe, Kluane Range, Yukon Territory, Canada. *Permafrost and Periglacial Processes* **16**: 261–275. DOI: 10.1002/ppp.530
- Mackay JR. 1983. Downward water movement into frozen ground, western Arctic coast, Canada. *Canadian Journal of Earth Sciences* **20**: 120–134.
- Matsumoto H, Ishikawa M. 2002. Gelifluction within a solifluction lobe in the Kärkevagge valley, Swedish Lapland. *Geografiska Annaler* **84A**: 261–265.
- Matsumoto H, Kurashige Y, Hirakawa K. 2001. Soil moisture conditions during thawing on a slope in the Daisetsu Mountains, Hokkaido, Japan. *Permafrost and Periglacial Processes* **12**: 211–218. DOI: 10.1002/ppp.364
- Matsuoka N. 1994. Continuous recording of frost heave and creep on a Japanese high mountain slope. *Arctic and Alpine Research* **26**: 245–254.
- Matsuoka N. 1998. The relationship between frost heave and downslope soil movement: field measurements in the Japanese Alps. *Permafrost and Periglacial Processes* **9**: 121–133.
- Matsuoka N. 2001. Solifluction rates, processes and landforms: a global review. *Earth-Science Reviews* **55**: 107–133.
- Matsuoka N. 2005. Temporal and spatial variations in periglacial soil movements on alpine crest slopes. *Earth Surface Processes and Landforms* **30**: 41–58.
- Matthews JA, Harris C, Ballantyne CK. 1986. Studies on a gelifluction lobe, Jotunheimen, Norway: 14C chronology, stratigraphy, sedimentology and palaeoenvironment. *Geografiska Annaler* **86A**: 345–360.
- Matthews JA, Seppälä M, Dresser PQ. 2005. Holocene solifluction, climate variation and fire in a subarctic landscape at Pippokangas, Finnish Lapland, based on

- radiocarbon-dated buried charcoal. *Journal of Quaternary Science* **20**: 533–548.
- Ripley AG. 2004. *An investigation of soil structure interaction resulting from the freezing and thawing of slopes*. Unpublished PhD thesis, University of Dundee.
- Smith DJ. 1988. Rates and controls of soil movement on a solifluction slope in the Mt Rae area, Canadian Rocky Mountains. *Zeitschrift für Geomorphologie, Supplementband* **71**: 25–44.
- Washburn AL. 1967. Instrumental observations of mass-wasting in the Mesters Vig district, Northeast Greenland. *Meddelelser om Grønland* **166**: 318 pp.
- Washburn AL. 1979. *Geocryology: a Survey of Periglacial Processes and Environments*. Edward Arnold: London.
- Washburn AL. 1999. A high Arctic frost-creep/gelifluction slope, 1981–89: Resolute Bay, Cornwallis Island, Northwest Territories, Canada. *Permafrost and Periglacial Processes* **10**: 163–186.